Available online at www.sciencedirect.com
SCIENCE DIRECT
Journal of Catalysis 233 (2005) 68–80
JOURNAL OF CATALYSIS
www.elsevier.com/locate/jcat

In situ diffuse-reflectance infrared spectroscopic investigation of promoted sulfated zirconia catalysts during *n*-butane isomerization

Barbara S. Klose, Friederike C. Jentoft *, Robert Schlögl

Department of Inorganic Chemistry, Fritz Haber Institute of the Max Planck Society, Faradayweg 4-6, 14195 Berlin, Germany

Received 8 January 2005; revised 24 March 2005; accepted 6 April 2005

Available online 23 May 2005

Abstract

Sulfated zirconia, unpromoted or promoted with either 2 wt% iron or manganese, was investigated by in situ diffuse reflectance IR spectroscopy during activation, *n*-butane isomerization (323–378 K, 1–5 kPa *n*-butane), and regeneration. During activation at 773 K in N_2 or O_2, more than 95% of the adsorbed water was removed, and comparison of the resulting pattern of sulfur–oxygen vibrations with DFT calculations (A. Hofmann and J. Sauer, J. Phys. Chem. B 108 (2004) 14652) suggests $S_2O_7^{2-}$ as a major surface species. All catalysts underwent an induction period before maximum rates were measured, which at 1 kPa *n*-butane were 350 and 180 μmol g^{-1} h^{-1} for the Fe- or Mn-promoted catalyst (323 K) and 5 μmol g^{-1} h^{-1} for sulfated zirconia (358 K). During isomerization several bands increased in the range of 1700–1600 cm^{-1}; the growth of a band at 1600 cm^{-1} was restricted to the period of increasing catalytic activity. The rate of isomerization was linearly correlated with the total area increase of the bands in this region, indicating that the absorbing species are either active surface intermediates or side products (possibly water) formed in an amount proportional to the active surface species. The rate per such species was much higher in the presence of Mn; that is, promoters facilitate reaction steps after the initial alkane activation. The promoted materials deactivated within hours under the applied conditions, but complete recovery of the spectral and catalytic properties of Mn-promoted sulfated zirconia was possible through regeneration in O_2 at 773 K. Attempts to regenerate in N_2 produced unsaturated surface species absorbing at 1532 and 1465 cm^{-1}.

Keywords: Sulfated zirconia; Iron; Manganese; Butane isomerization; Deactivation; Regeneration; DRIFT spectroscopy; In situ

1. Introduction

Sulfated zirconia (SZ) is a highly active catalyst for the skeletal isomerization of alkanes at low temperature (e.g., *n*-butane is isomerized at room temperature) [1]. The performance of SZ can be improved by the addition of first-row transition-metal cations. Among the most intensely studied promoters are iron and manganese, in combination [2–29], and as single promoters [6,20,25,29–32], whereby some authors could not find a promoting effect for manganese [9,25,29]. Initially, the promoters were believed to enhance acidity [21], but this idea had to be dismissed [12,16,17]. It could be shown that manganese and iron are incorporated at least in part into the zirconia lattice [33], but it is not clear whether and how they participate in alkane activation and reaction.

A frequently voiced hypothesis attributes a redox function in the reaction initiation to the promoters [3,23,26,27], and as evidence, a more active material after activation in oxidizing atmosphere than after activation in inert gas has been put forth by Wan et al. [27] and by Song and Kydd [23] for mixed Fe, Mn-promoted catalysts. It has been suggested that butane is activated through oxidative dehydrogenation (ODH) to give water and butenes, which are easily protonated to carbenium ions, which serve as reaction chain carriers [27]. In addition to the optimal activation atmosphere, the activation temperature has been discussed, mainly in the context of water content. Vera et al. [34] reported increasing activity of SZ with higher activation temperatures for the range less than 898 K. Song and Kydd inferred that the

* Corresponding author.
E-mail address: jentoft@fhi-berlin.mpg.de (F.C. Jentoft).

0021-9517/$ – see front matter
doi:10.1016/j.jcat.2005.04.011

Brønsted-to-Lewis ratio should be adjusted to 2:1 by hydration in SZ [35]; the best pretreatment temperatures were 423 K for SZ and 723 K for promoted SZ [23]. Closely linked to the hydration degree is the state of a key component of these catalysts, the sulfate, as indicated by a shift of the S=O vibration with variation of the activation temperature [58].

Evidence for the formation of water or carbenium ions as a consequence of ODH is lacking, but deactivation has been explained by reduction of the promoter for Fe-promoted SZ by Millet et al. [36] However, Yamamoto et al. [6] reported that the valence of Fe was unaffected by *n*-butane. Mn reacted upon exposure to butane [6], but not in a way that is correlatable with catalytic performance [37,38]. Deactivation of promoted SZ catalysts may also be caused by effects that have been proposed to account for deactivation [39–42] of SZ itself, such as coke formation [34,41,43–54] (excluded by other authors [55]), reduction of Zr^{4+} [34], loss of sulfur [50,54,56] zirconia phase transformation [57], and poisoning by water [34,58].

Attempts to regenerate SZ catalysts have been made under conditions resembling those of activation. Reactivation of SZ is possible in air or oxygen at 723–753 K, and the DRIFT, Raman, or UV–vis spectra are identical to those of the fresh catalyst [47,48,51]. Risch and Wolf [40] obtained better results when they not only regenerated the catalyst in O_2 but also exposed it to water. Coke can be removed from the surface as CO_2 in inert gas, but the sulfate decomposes concomitantly [34,49]. Coke removal under oxidative conditions may disguise the fact that the catalyst is also oxidized.

Many of the investigations of catalyst activation and regeneration just report the influence of different treatments on the activity without characterization of the catalyst in the activated state. Moreover, studies of interaction of SZ catalysts with alkanes using IR [59–61], EPR [62], or calorimetry [63] lack information on the gas-phase composition and potential reactions. Thus initiation of the reaction by ODH [27], with concomitant reduction of the promoter [27] or the sulfate and zirconium [34], and water formation [27,34] is so far a hypothesis. Furthermore, most ideas on deactivation are based on the study of the catalysts after they are removed from the reactor. There are few true in situ data with simultaneous analysis of SZ catalysts and their butane isomerization performance with time on stream [37,38,64], and the potential formation of water and the state of sulfate during the reaction have not yet been addressed.

We present an in situ IR study, using the diffuse-reflectance technique to avoid having to press a wafer, which may cause partial transformation of tetragonal to monoclinic zirconia and reduces activity [65]. SZ, Fe-promoted, and Mn-promoted SZ are compared after activation and during *n*-butane isomerization. To complement our in situ X-ray absorption work [37,38], Mn-promoted SZ was selected to investigate activation and regeneration treatments in oxidizing or inert atmosphere.

2. Experimental

2.1. Catalyst preparation

Sulfated zirconium hydroxide (MEL Chemicals; MEL XZO 682/01) served as a precursor. According to the manufacturer, it contains $(NH_4)_2SO_4$ equal to an SO_3 content of 5–6 wt% on the ZrO_2 content of 70–80%. Before further processing (impregnation or thermal treatment) the material was dried for 21 h at 383 K and cooled to room temperature in a desiccator. Promoters were introduced via the incipient wetness method. Aqueous solutions of either $Fe(NO_3)_3 \cdot 9H_2O$ or $Mn(NO_3)_2 \cdot 4H_2O$ (both p.a. Merck, Darmstadt) were added dropwise with vigorous stirring in a porcelain mortar; 4 ml solution per 10.9 g powder was always used. The solution concentration was chosen such that the final promoter content, estimated on the basis of TG measurements showing that 74% of the precursor remained after thermal treatment as "sulfated zirconia," was 2.0 wt% metal. Calcination was performed in 20–25-g portions in a quartz boat with a volume of 17.1 ml, which was placed in a quartz tube that was purged with 200 ml min^{-1} of synthetic air ("hydrocarbon-free"; Linde) [66]. The temperatures were selected according to recommendations in the literature; good performance is reported for unpromoted sulfated zirconia after calcination at 823 K [58] and for promoted sulfated zirconia after calcination at 923 K [23]. The heating and cooling ramps (as far as possible) were 3 K min^{-1}, and the holding time at either 823 K (SZ) or 923 K (MnSZ, FeSZ) was 3 h.

2.2. Diffuse-reflectance Fourier transform infrared spectroscopy

A Bruker IFS 66 FTIR spectrometer at a spectroscopic resolution of 1 cm^{-1}, a diffuse-reflectance attachment ("The Selector" from Graseby Specac), and a D315M MCT detector were used. The spectrometer was purged with purified air. Reactions were conducted in a 2.5-mm-tall gold cup with 8.5-mm OD and 7.2-mm ID placed in a Graseby Specac "Environmental Chamber" with a ZnSe window. There was no flow through the bed; gas exchange occurred by convection and diffusion. The top part of the bed is analyzed with IR radiation. Spectra were taken with the use of KBr under N_2 purging as a reference. Parameters for spectrum acquisition and calculation were as follows: 100 scans, single-sided fast return interferogram, Blackman–Harris 3-term apodization function.

2.3. Catalyst activation and regeneration

About 160 mg of catalyst was placed in the gold cup for DRIFTS, or 500 mg of catalyst was placed in a once-through plug–flow fixed-bed reactor made of glass with a 12-mm inner diameter and a frit to support the catalyst. The activation temperature in the tubular reactor was 723 K. In the

DRIFTS cell, a nominal temperature of 773 K was selected, which corresponds to a somewhat lower temperature of the surface of the catalyst bed due to placement of the heater and control thermocouple in the cell. The samples were heated at 25 K min^{-1} to the activation temperature in a flow of either 48 ml min^{-1} N_2 (5.0, Linde, further purified with Oxysorb and Hydrosorb cartridges; Messer-Griessheim) or 24 ml min^{-1} O_2 (Linde; Hydrosorb), held at the desired temperature for 30 min, and then cooled to the reaction temperature. Regeneration was performed analogously to activation.

2.4. Reaction conditions and analysis

Reactions were conducted at 358 or 378 K (SZ) and at 323 K (Fe-, Mn-promoted samples). The *n*-butane partial pressure in the reaction mixture was either 1 or 5 kPa; the balance was nitrogen; these concentrations were achieved with the use of a purchased mixture of 5 vol% *n*-butane (3.5, Linde) in nitrogen, which was optionally diluted with N_2. The feed was not further purified; the only detectable impurity (GC-FID) was isobutane. The flow through the in situ DRIFTS cell was 30 ml min^{-1}, and the flow through the tubular reactor was 100 ml min^{-1}, all at atmospheric pressure. Reaction products were analyzed by on-line gas chromatography (Varian 3800) with a SilicaPLOT capillary column (length 60 m, 0.32 mm ID, film thickness 4 μm, Chrompack) and flame ionization detection.

3. Results

3.1. Catalyst characterization

In all catalyst samples, only the tetragonal phase could be detected by X-ray diffraction. N_2 BET surface areas were SZ 155 m^2 g^{-1}, FeSZ 139 m^2 g^{-1}, and MnSZ 112 m^2 g^{-1}.

3.2. Activation in N_2 and n-butane isomerization

IR spectra of the calcined, not yet activated catalysts are typical of a hydrated surface with strong hydrogen bonding vibrations. As an example, the initial spectrum of MnSZ is shown in Fig. 1. The figure also contains spectra of SZ, MnSZ, and FeSZ taken after activation in nitrogen flow at 773 K. The spectra were taken after the catalysts were cooled to reaction temperature, that is, at 358 K for SZ and at 323 K for FeSZ and MnSZ. The activation procedure results in strong reduction of the broad band between 3700 and 3000 cm^{-1}, consistent with dehydration. The spectra are characterized by bands originating from hydroxyl groups and adsorbed water (3700–3500 and 1630–1600 cm^{-1} ranges), from different sulfate structures (2800–1950 cm^{-1} and 1400–1000 cm^{-1} ranges), and from adsorbed nitrogen (2336 cm^{-1}). The positions of the bands are listed in Table 1. The three catalysts show similar but not identical spectra. The spectrum of SZ exhibits an additional

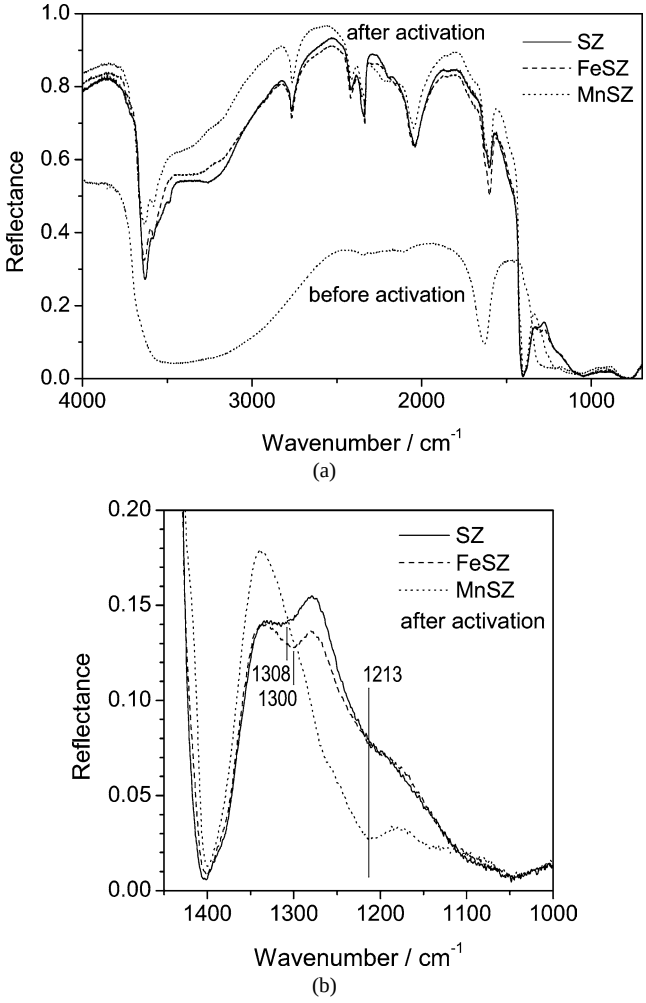

Fig. 1. Diffuse reflectance IR spectra of SZ, MnSZ, and FeSZ recorded at 323 K (358 K SZ) before (only MnSZ) and after activation in N_2 at 773 K. (a) Complete spectrum; (b) enlargement of range between 1450 and 1000 cm^{-1}. Band positions in Table 1.

band at 3489 cm^{-1} (Fig. 1a). In the range below 1450 cm^{-1} (shown in Fig. 1b), the spectra of SZ and FeSZ are comparable, and the spectrum of MnSZ differs. Bands at 1308 (SZ) and 1300 cm^{-1} (FeSZ) cannot be discerned in the spectrum of MnSZ, which, on the other hand, shows much more intense absorptions at 1213 and around 1145 cm^{-1} than the two other catalysts.

First, data from catalytic experiments in the in situ DRIFTS cell are compared with those generated with a tubular fixed-bed plug-flow reactor. *n*-Butane isomerization in the two systems was performed at 323 K with the MnSZ catalyst and the same weight hourly space velocity of 0.3 h^{-1}. Fig. 2a shows the isobutane formation rates with time on stream. Qualitatively, the same reaction profile is observed, consisting of an induction period, a maximum in activity, and a deactivation period. The maximum rate is somewhat lower in the DRIFTS cell and is achieved about 15 min later than in the tubular reactor. The considerable dead volume of the DRIFTS cell (ca. 100 ml) may account for this delay, be-

Table 1
Band positions from DRIFT spectra recorded at reaction temperature after activation at 773 K in N_2

SZ	FeSZ	MnSZ	Assignment
3630	3634	3638	Triply bridged ν(OH) next to $S_2O_7^{2-}$
3582	3581	3581	$\nu(H_2O_{ads})$ next to SO_4^{2-}
3489	–	–	Triply bridged ν(OH) on dehydrated ZrO_2
2767	2767	2761	Overtone of vibration around 1400 cm^{-1}
2416	2418	2415	Combination of vibrations at 1400/1050 cm^{-1}
2341	ca. 2345	ca. 2345	Overtone of vibration around 1213 cm^{-1}
2336	2336	2336	$\nu(N_{2,ads})$
2190		2220	Overtone or combination mode of ν(S–O)
2040	2042	2046	Overtone of vibration around 1050 cm^{-1}
1625	ca. 1625	ca. 1625	$\delta(H_2O_{ads})$
1603	1597	1597	$\delta(H_2O_{ads})$
1402	1400	1399	ν(S=O) of $S_2O_7^{2-}$, $S_2O_7^{2-} \cdot H_2O$ or $SO_{3,ads}$
1378 sh	1375 sh	(sh)	ν(S=O) of $S_2O_7^{2-}$ or SO_4^{2-}
1308	1300		ν(S=O) of $S_2O_7^{2-} \cdot yH_2O$
(1211)	1211	1213	ν(S–O) of $S_2O_7^{2-}$ or $S_2O_7^{2-} \cdot yH_2O$
		1145	ν(S–O) of $S_2O_7^{2-} \cdot yH_2O$
1050	1050	1050	ν(S–O) of $S_2O_7^{2-}$ or $SO_{3,ads}$
Additional bands after 15 h on stream (recorded in feed flow)			
2966	2966	2966	ν(CH)
2939	2939	2939	ν(CH)
2877	2877	2877	ν(CH)
1466	1466	1466	δ(CH)
		1300	ν(S=O) of $S_2O_7^{2-} \cdot yH_2O$

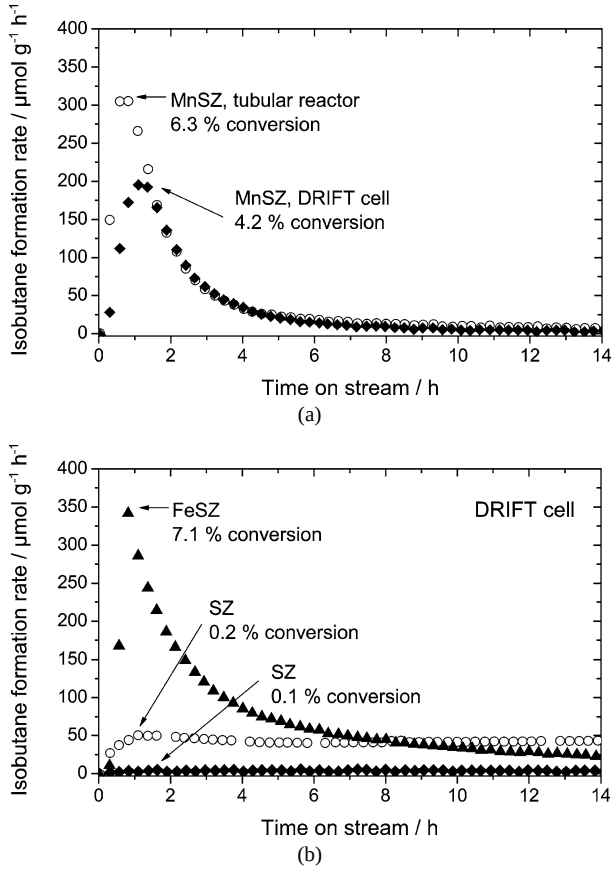

Fig. 2. Rate of isomerization vs time on stream after activation in N_2. (a) MnSZ at 323 K, 1 kPa *n*-butane, and WHSV 0.3 h^{-1}; (b) ◆, SZ at 358 K and 1 kPa *n*-butane; ○, SZ at 378 K and 5 kPa *n*-butane; ▲, FeSZ at 323 K and 1 kPa *n*-butane. Maximum conversions indicated.

cause some time is needed to generate the desired *n*-butane partial pressure of 1 kPa (1 vol% *n*-butane in nitrogen). Certainly, the reaction data from the DRIFTS cell reflect the essential performance features of the catalyst and are of sufficient quality.

Fig. 2b gives the *n*-butane isomerization rates for the other two catalysts, SZ and FeSZ, measured in the DRIFTS cell. SZ exhibited no measurable activity at 323 K (not shown), and even at 358 and 378 K (Fig. 2b), the maximum rates are lower than those for FeSZ or MnSZ at 323 K. FeSZ produces a higher maximum isomerization rate (>350 µmol g^{-1} h^{-1}) than MnSZ (200 µmol g^{-1} h^{-1}). The promoted catalysts deactivate partially within hours, the MnSZ more rapidly than the FeSZ catalyst. At the low conversions achieved with SZ, hardly any deactivation is observed. The long-term activity (>10 h) is seemingly highest for SZ; but the reaction temperature is 55 K above that used for the promoted systems.

IR spectra recorded for MnSZ during *n*-butane isomerization are shown in Figs. 3a and 3b. Within the first minute on stream, bands at 2966, 2939, 2877 (CH stretching), and 1466 cm^{-1} (CH bending) become visible. The following spectra represent the situation during the induction period at ca. 2% conversion, at maximum conversion (4.2%), during deactivation at about 2% conversion, and after 15 h time on stream. During the course of the reaction the overall reflectance between 4500 and 1200 cm^{-1} decreases. Further changes include growth of a band at around 5200 (not shown), which is indicative of adsorbed water. Additional bands develop in the region of 1630–1600 cm^{-1}. The OH stretching band at 3580 cm^{-1} increases in intensity and

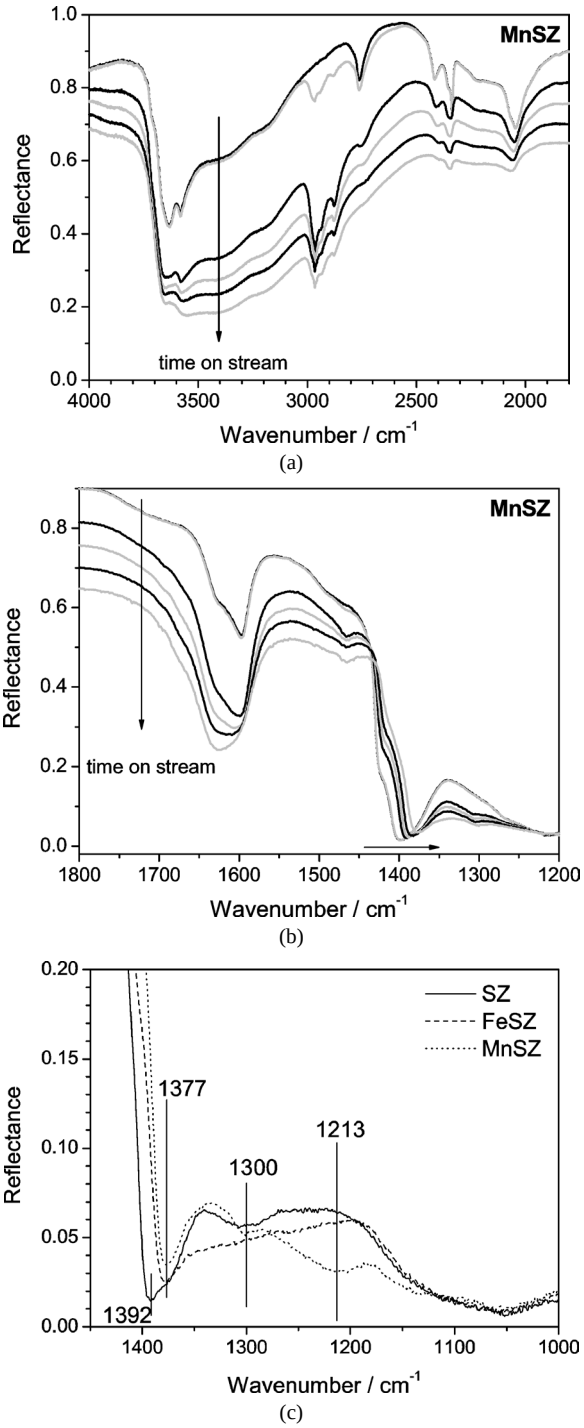

Fig. 3. Diffuse reflectance IR spectra of (a) and (b) MnSZ acquired at different times on stream (0, 1, 34, 65, 144 min, and 15 h) during *n*-butane isomerization at 323 K; (c) SZ (358 K), FeSZ, and MnSZ after 15 h on stream.

broadens. The band of adsorbed N_2 at 2336 cm^{-1} disappears during the induction period. While the isomerization reaction progresses, the S=O band at 1399 cm^{-1} is slowly shifted to 1377 cm^{-1} (Fig. 3b).

Changes in the spectra of SZ and FeSZ observed during *n*-butane isomerization are, in principle, the same as those for MnSZ. Differences can only be discovered in the region

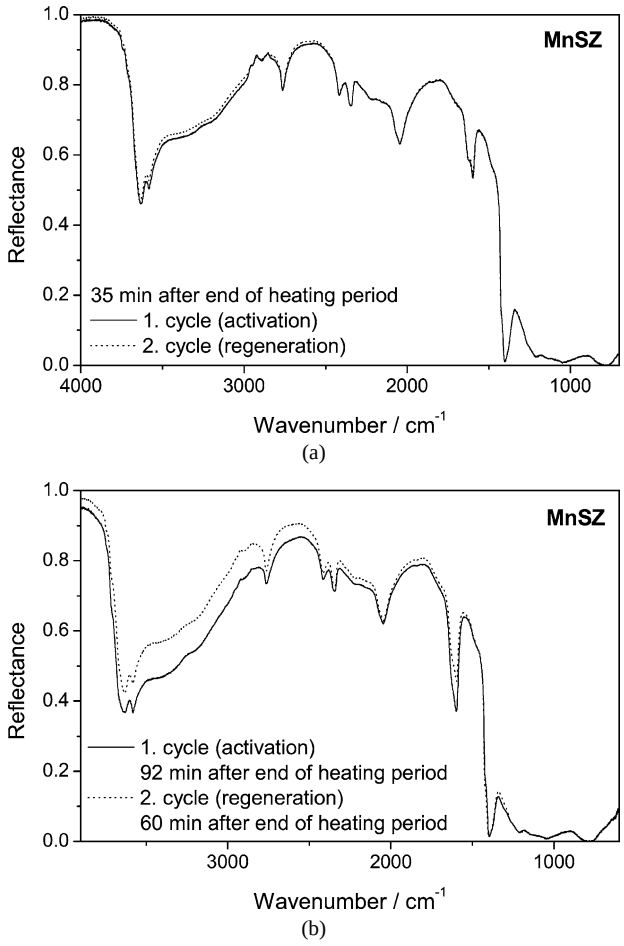

Fig. 4. Diffuse reflectance IR spectra of MnSZ after initial activation and after regeneration in O_2. (a) 35 min after end of heating period; (b) before start of reaction.

between 1450 and 1000 cm^{-1}, as spectra taken after 15 h of reaction show (Fig. 3c). Whereas the spectra of SZ and FeSZ remain unaffected in this region besides the shift of the vibration at ≈ 1400 cm^{-1}, a band at around 1300 cm^{-1} is formed in the case of MnSZ.

3.3. Activation and regeneration of manganese-promoted sulfated zirconia in N_2 and O_2

MnSZ, which exhibits distinct induction and deactivation periods at 323 K, was chosen for regeneration experiments. Fig. 4a shows the IR spectra of a MnSZ catalyst at 323 K after activation and after its regeneration in flowing 100% O_2 after 16 h of isomerization reaction at 323 K. These spectra were recorded 35 min after the end of the holding time at 773 K, that is, during the cooling phase. The band positions in the two spectra are identical, and the intensities differ only slightly in the region of OH stretching and deformation vibrations and between 3500 and 3000 cm^{-1}. The waiting time after cool-down determined the catalyst state immediately before the start of the reaction. Fig. 4b shows spectra acquired 92 min and 60 min after the end of the heating period at 773 K. The longer waiting time in O_2 flow

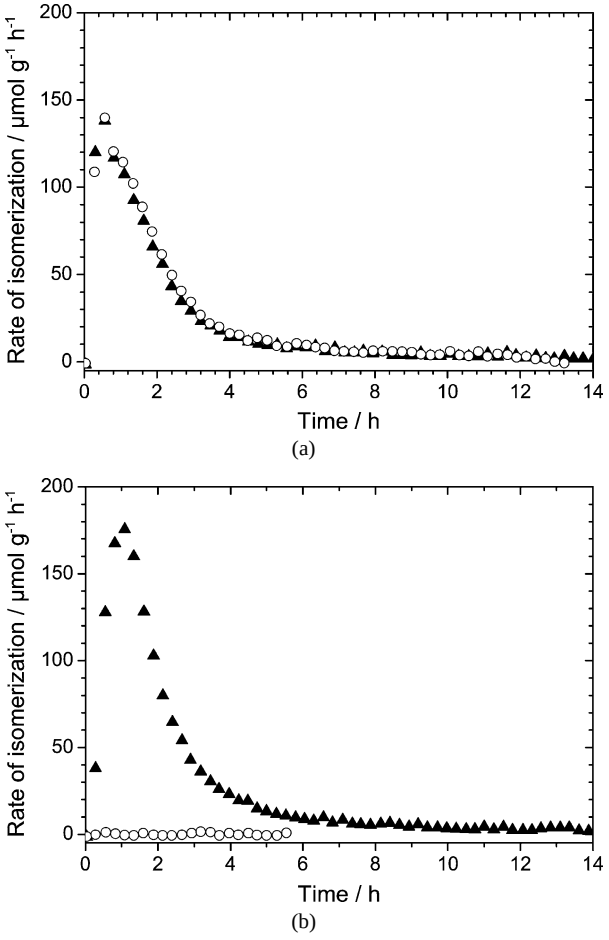

Fig. 5. Rate of isomerization vs time on stream of MnSZ at 323 K and 1 kPa *n*-butane after initial activation and after regeneration. (a) ▲, after activation in O_2; ○, after regeneration in O_2; (b) ▲, after activation in N_2; ○, after "regeneration" in N_2.

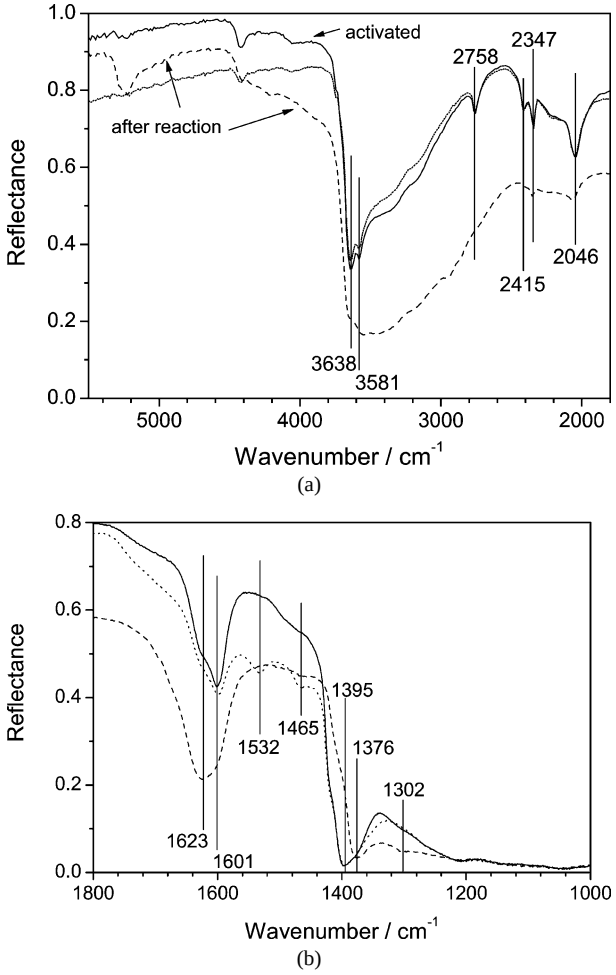

Fig. 6. Diffuse reflectance IR spectra of MnSZ recorded at 323 K in N_2: (—) after activation at 773 K; (- - -) after 16 h reaction at 323 K and 1 kPa *n*-butane and 1 h of purging with N_2; (· · ·) after "regeneration" at 773 K. (a) Range 5500–1800 cm^{-1}; (b) range 1800–1000 cm^{-1}.

after the initial activation in comparison after the regeneration leads to higher intensities of the water deformation bands (around 1600 cm^{-1}) and the bands caused by hydrogen bridges (3500–3000 cm^{-1}). This difference in the water content has no discernible influence on the rate of isomerization, as can be seen in Fig. 5a, which shows the corresponding rate data. The MnSZ catalyst can be fully regenerated with the same reaction profile versus time on stream. With the use of a 100% O_2 atmosphere, it is possible to regenerate the catalyst at least twice. Also after initial activation in N_2, regeneration in 100% O_2 produces the same catalyst state as in the experiment with both activation and regeneration in O_2.

Activation in N_2 seems to produce a slightly more active MnSZ catalyst than activation in 100% O_2 (compare Figs. 5a and 5b); the maximum rate reaches 180 µmol g^{-1} h^{-1} versus only 140 mmol g^{-1} h^{-1} after activation in O_2. However, the activity changes so rapidly that the time resolution of the GC analysis may be insufficient to detect the real maximum. In a 100% N_2 atmosphere, a deactivated MnSZ catalyst cannot be regenerated; it is completely inactive (Fig. 5b). Fig. 6 shows, in two sections, the spectra of MnSZ after activation, after reaction and purging of the cell with nitrogen for 1 h, and after a regeneration attempt at 773 K in N_2. The spectrum after reaction exhibits bands indicative of adsorbed water, including hydrogen bridges. A group of weak absorption bands between 2980 and 2850 cm^{-1} could arise from surface hydrocarbon deposits. The post-reaction heating in N_2 does not lead to a complete recovery of the spectrum of the activated sample. Instead, two new bands appear in the CH deformation region of aliphatic and aromatic compounds at 1532 and 1465 cm^{-1} (Fig. 6b). However, all bands arising from OH groups or sulfate species approach their original position and intensity.

4. Discussion

4.1. Estimation of water content after activation

The main effect of activation that is visible in the IR spectra is dehydration. The bands indicative of hydrogen bridges in the range of 3500–3000 cm^{-1} are reduced in in-

tensity, as are the water deformation modes in the range of 1630–1600 cm^{-1}. Thermogravimetry (TG) experiments with a number of promoted and unpromoted samples (stored in vials in the laboratory) show varying water contents, typically in the range of 2.2–4.6 wt%, corresponding to 1.2–2.5 mmol g^{-1}. A rough estimate of the amount of water removed during activation is given by the intensity of the bands in the region of 1630–1600 cm^{-1}. The reflectance spectra were converted into Kubelka–Munk units, and integration was performed over the width of the entire feature. For SZ, MnSZ, and FeSZ, the intensity was reduced by >95% after activation at 773 K. The remaining water content was then estimated to be 60–125 μmol g^{-1}. The typical sulfur content (also from TG experiments) is about 560 μmol g^{-1}, meaning that in the activated catalysts, enough water is present to hydrate a considerable fraction of the sulfate species. For example, about 10–22% of SO_4^{2-} or 20–44% of $S_2O_7^{2-}$ groups (pyrosulfate) could be singly hydrated.

4.2. Interpretation of spectra of activated catalysts

Recently, DFT calculations of the vibrational spectra of sulfated zirconia have become available [67,68]. Hofmann and Sauer investigated the stability and spectral signature of various sulfate structures in combination with different water contents on the (101) surface of the tetragonal phase. The (101) surface is the most stable one, according to the calculations by Hofmann and Sauer; however, Benaissa et al. [69]. identified the (110) plane as most abundant with high-resolution electron microscopy. Morterra et al. reported "low Miller-index crystal planes" [70]. Our catalysts are tetragonal, and although the facet planes are unknown, experimental and calculated frequencies can be compared to assist interpretation.

A number of bands arise from S=O and S–O vibrations. According to the calculations, some of them are characteristic: only S=O vibrations of $S_2O_7^{2-}$ species, which may be hydrated, or of adsorbed SO_3, or of tridentate SO_4^{2-} yield band positions above 1395 cm^{-1}. Bands at 1400 cm^{-1} and above have been assigned previously to $S_2O_7^{2-}$ by Bensitel et al. [71] and Morterra et al. [72]. We observed that the S=O band was shifted upward during activation with progressing dehydration. Positions given in the literature depend on the degree of hydration. Other interpretations can also be found; Riemer et al. [73] interpreted a band at 1382 cm^{-1} as tridentate monosulfate.

According to DFT results the bands at 1308–1300 cm^{-1}, detected for SZ and FeSZ, may arise from S=O vibrations of SO_4^{2-} on a strongly hydrated surface or of $S_2O_7^{2-}$ on a slightly hydrated surface. Another S=O vibration located at 1213 cm^{-1} (very intense for MnSZ) also originates from a possibly hydrated $S_2O_7^{2-}$ species. A hydrogen bridge to a neighboring OH group causes the (for a double bond) relatively low frequency. The bands at 1145 and 1050 cm^{-1} are clearly S–O bond vibrations, and again several interpretations are possible. The band at 1145 cm^{-1} falls in the range of S–O vibrations of SO_4^{2-} on a strongly hydrated surface or of $S_2O_7^{2-}$ on a weakly hydrated surface; the band at 1050 cm^{-1} could be assigned to $S_2O_7^{2-}$ on a dehydrated surface or to adsorbed SO_3. According to the spectra and the above estimation of the water content, the surface is still hydroxylated after activation but only moderately hydrated. It therefore seems appropriate to exclude the presence of SO_4^{2-} species on a richly hydrated surface. $S_2O_7^{2-}$ species are definitely present on all three catalysts, and the nearest surroundings of these species sometimes feature adsorbed water. In comparison with the two other samples, MnSZ features more of the $S_2O_7^{2-}$ species absorbing at 1213 cm^{-1}. Since all samples have about equal sulfate content, MnSZ should then have lower concentrations of other sulfate species. Weaker in the spectrum of MnSZ than in those of SZ and FeSZ is the band at 1300–1308 cm^{-1}, which belongs to the "pyrosulfate with adjacent water" configuration. Given the slightly better dehydration of MnSZ (see the range 3500–3000 cm^{-1} in Fig. 1a), the band at 1213 cm^{-1} may be assigned to a dehydrated pyrosulfate state.

More bands due to S=O and S–O vibrations are observed. The bands at 2767, 2345, and 2040 cm^{-1} are assigned to overtones of the vibrations at around 1400, 1213, and 1050 cm^{-1}. The band at 2416 cm^{-1} is believed to be a combination mode of the bands at 1400 and 1050 cm^{-1}.

The two bands at about 3635 and 3580 cm^{-1} (all samples) are OH-stretching vibrations. In the promoted materials, the higher frequency band appears to be less intense relative to the lower frequency band. Babou et al. [60] reported a band at 3645 cm^{-1} for sulfated zirconia and at 3665 cm^{-1} for nonsulfated zirconia. Morterra et al. [74] attributed a band at 3640 cm^{-1} to "free surface OH groups of the ZrO_2 system" because its position and behavior upon dehydration resemble those of a band of nonsulfated zirconia. Riemer et al. [73] observed a band at 3640 cm^{-1} only when sulfate was present and favored the idea of an OH group bridging sulfur and zirconium. The spectrum of gas-phase sulfuric acid exhibits vibrations of S–OH groups at 3609 cm^{-1}. The bands in the spectra of SZ, FeSZ, and MnSZ are at 3630–3638 cm^{-1} and thus are located in the range between the OH bands of pure zirconia and sulfuric acid.

For the band at 3630 cm^{-1} several possibilities emerge from the calculations, some of which can be excluded because of a lack of plausibility, such as a richly hydrated zirconia surface. It is not possible to distinguish from the positions between scenarios involving either SO_4^{2-} (dehydrated or highly hydrated) or $S_2O_7^{2-}$ species (dehydrated or singly hydrated). In light of the sulfur-oxygen vibrations, which suggest $S_2O_7^{2-}$ to be the predominant species, a triply bridged OH group next to $S_2O_7^{2-}$ is the best interpretation.

The vibration at 3580 cm^{-1} is characteristic for a surface with SO_4^{2-} species and originates from adsorbed water. The band at 3489 cm^{-1}, which does not appear in the spectra of the promoted samples, is similar to a band observed at

3510 cm^{-1} for a sulfate-free mixture of tetragonal and monoclinic zirconia (ca. 1:3) and can be attributed, with the help of the DFT calculations, to triply bridged OH groups on a dehydrated zirconia surface.

The two bands at about 1625 and 1600 cm^{-1} are attributable to deformation vibrations of adsorbed water, indicating that the surface is not completely dehydrated during activation. A value of 1600 cm^{-1} results from DFT calculations only for water configurations on a sulfated but not on a pure zirconia surface. The band at 1625 cm^{-1} is nonspecific, according to the calculations; it is not observed for unsulfated zirconia, and thus the corresponding water species should be associated with a sulfate species.

The band at 2336 cm^{-1} (overlapping with the band at 2040 cm^{-1}) is noticeably sharper than the sulfate overtones and combination modes, appears only when nitrogen is used for activation, and is located slightly above the gas-phase frequency for nitrogen of 2330 cm^{-1} [75]. It is therefore assigned to the stretching vibration of adsorbed nitrogen. This band is absent after activation in O_2; instead a band at $\approx$ 1595 cm^{-1} (hidden beneath the OH deformation bands) indicates the presence of adsorbed O_2 [76] (gas-phase frequency 1556 cm^{-1} [75]).

In summary, a comparison of calculated and measured frequencies clearly points to $S_2O_7^{2-}$ as the prevailing surface species on the activated samples; single water molecules are often nearby. Evidence for other species such as SO_4^{2-} is only indirect, through OH stretching vibrations, and the data for the sulfur-oxygen region do not favor this interpretation. The presence of $S_2O_7^{2-}$ on the surface of zirconia among other species has been inferred before [71,72]. Bensitel et al. [71] observed an increasing fraction of $S_2O_7^{2-}$ for samples with increasing sulfur content from 250 to 500 µmol g^{-1}. SZ, MnSZ, and FeSZ contain about 560 µmol g^{-1} sulfur. Their spectra differ slightly, but are all dominated by the pattern of $S_2O_7^{2-}$.

4.3. Activation and catalytic performance

By choice of the activation conditions, the degree of hydration of the surface and the oxidation states of individual catalyst components are determined. As discussed above, the surface of our catalysts was more than 95% dehydrated. In this activated state, the surface is highly hydrophilic and adsorbs traces of water from the environment. Different waiting times in O_2 after cool-down to reaction temperature led to variations in the band intensity in the range of 1630–1600 cm^{-1}; the areas and thus the water content of MnSZ corresponded to either 2.5 or 5% of the initial area (Fig. 4b). The influence of the activation conditions, which determine the surface hydration, has been stressed in several papers [39,40,48,58,63,77]; González et al. [78] inferred that a water concentration of 75 µmol g^{-1} is optimal, whereas Song and Kydd [35] reported the best performance to occur at 200 µmol g^{-1}. We did not find any effect of a variation by a factor of 2 in the degree of hydration on the catalytic performance (Figs. 4b and 5a).

The atmosphere during activation does not seem to have an influence on the performance of SZ [23]. More investigations are available for catalysts promoted with Fe and Mn, because of the potential redox function ascribed to the promoters. Wan et al. [27] found an effect of the atmosphere on the activity of Fe- and Mn-promoted SZ only for activation temperatures above 723 K; a treatment in air resulted in a conversion twice as high as that resulting from a treatment in He at 923 K. Morterra et al. [3] observed a promoting effect of Fe and Mn only after activation in air and not after activation in He. Song and Kydd [23] found a higher conversion after activation in air than after activation in He, regardless of the activation temperature (range ca. 523–873 K). After activation in N_2, our Fe- or Mn-promoted catalysts both exhibited, even at lower temperature, much higher maximum rates than sulfated zirconia. Activation of promoted catalysts in inert environment is thus possible, consistent with the observations of Wan et al. [27] and Song and Kydd [23]. SZ-based catalysts usually have been calcined in air at about 823–923 K, so there is no reason to expect further oxidation during an air treatment at lower temperature; rather, the presence of oxygen may prevent some reduction in comparison with heating in an inert atmosphere.

MnSZ activated in 100% O_2 produced a maximum rate of 140 µmol g^{-1} h^{-1} isobutane versus 180 µmol g^{-1} h^{-1} after activation in N_2. This difference was reproducible. However, errors could arise from lack of time resolution in the GC analysis (Fig. 5); specifically, a rapid increase in conversion for the O_2-activated sample may have been missed. A positive effect of an oxidizing activation is expected if a high oxidation state of the catalyst components is advantageous, that is, in a reaction initiation through oxidative dehydrogenation with, for example, the promoters as oxidizing agents, or if more sites become available through removal of ubiquitous surface carbon contaminations. Data for the changes in the promoter valence as a consequence of potential ODH are controversial. Millet et al. [36] applied X-ray photoelectron spectroscopy and found Fe to be reduced after *n*-butane isomerization at 323 K, but we could not find a performance-related change in the Mn valence with in situ X-ray absorption experiments at 333 K [37,38]. However, activation of MnSZ in 50% O_2 in He produced a catalyst with a better performance than did activation in He [38], which is similar to the trend reported in the literature for mixed Fe, Mn-promoted systems. All studies in the literature were conducted with air; the treatment in the present study was 100% O_2. Despite these extremes, namely 0 and 100% O_2, in the activation of MnSZ, the short-term isomerization rates were within close range and the long-term (6–14 h on stream) rates were almost the same for the two atmospheres. Hence, for the steady-state performance, the choice of activation atmosphere might be irrelevant. A systematic study of the influence of O_2 exposure, determined by partial pressure and duration of treatment, on maximum activity and

long-term performance of SZ catalysts is under way in our laboratory.

4.4. IR spectra during n-butane isomerization

The bands in the IR spectra arise from four different classes of species, that is, adsorbed hydrocarbon species, adsorbed N_2 (present after activation in N_2), OH groups and adsorbed water, and sulfate groups. During reaction, the spectral signature changes, and we attempted to determine whether changes in one species are connected to changes in another species or to the catalytic performance.

The dominant contributions in the regions of hydrocarbon vibrations arise from gas-phase species, as experiments with a nonreactive reference material (KBr) revealed. It has not been possible so far, for example, via the calculation of difference spectra, to identify bands attributable to adsorbed hydrocarbon species in the spectra recorded during butane isomerization.

The sharp band at 2336 cm^{-1} that is observed only after activation in N_2 is blue-shifted slightly versus the N_2 gas-phase absorption (2330 cm^{-1}), as is typical of N_2 interacting with acid sites [79]. At room temperature, N_2 is expected to interact with strong Lewis acid sites and not with OH groups. The band disappears during the induction period. The feed contains 95–99% N_2, so desorption due to reduced N_2 pressure in the gas phase is negligible. For nonsulfated zirconia, only a broad feature at 2341 cm^{-1} is observed, and it does not undergo significant changes during *n*-butane exposure (not shown). In light of these observations it can be concluded that *n*-butane or its reaction products displace N_2 adsorbed on strongly acidic Lewis sites on the surface of sulfated zirconia materials.

Further distinct changes occur in the region of 1760–1540 cm^{-1}. Two small bands at about 1600 and 1625 cm^{-1} are already present in this region after activation. These bands increase somewhat with time, also in the absence of butane, because water is present as a trace contaminant in the system and adsorbs to the catalyst. During *n*-butane isomerization, several intense bands develop rapidly with time on stream, shown for SZ and Mn-promoted SZ in Figs. 7a and 7b after conversion to Kubelka–Munk units and subtraction of a linear background. Bands in this region can arise from the deformation vibration of water, which in gas-phase water is observed at 1595 cm^{-1} but is shifted to higher wavenumbers when water is hydrogen-bonded to surface atoms or other water molecules. Alternatively, C=C stretching vibrations can absorb within this range. A band simultaneously growing at 5200 cm^{-1} is a combination mode of OH stretching and bending vibration and indicates the formation of water; however, contributions from other species cannot be excluded on the basis of our spectra. The broad feature between 1760 and 1540 cm^{-1} was fit with up to four Gauss curves (see, for example, Fig. 7c). Band positions were at 1720–1685, 1680–1655, 1635–1620, and 1605–1598 cm^{-1}. An area of zero sometimes resulted for the bands at 1720–1685 and 1680–1655 cm^{-1}, depending on the constraints applied during the fitting procedure. All bands grew with time on stream, and when the full width at half-maximum was fixed (e.g., to 27 cm^{-1}), scatter was reduced and the increase was monotonic. The areas of the other two (three) bands in the range of 1690–1625 cm^{-1} first increased steeply for about 2 h and then more slowly. The band at 1600 cm^{-1} increased during the induction period and then ceased growing, which can also be recognized in the spectra in Figs. 7a

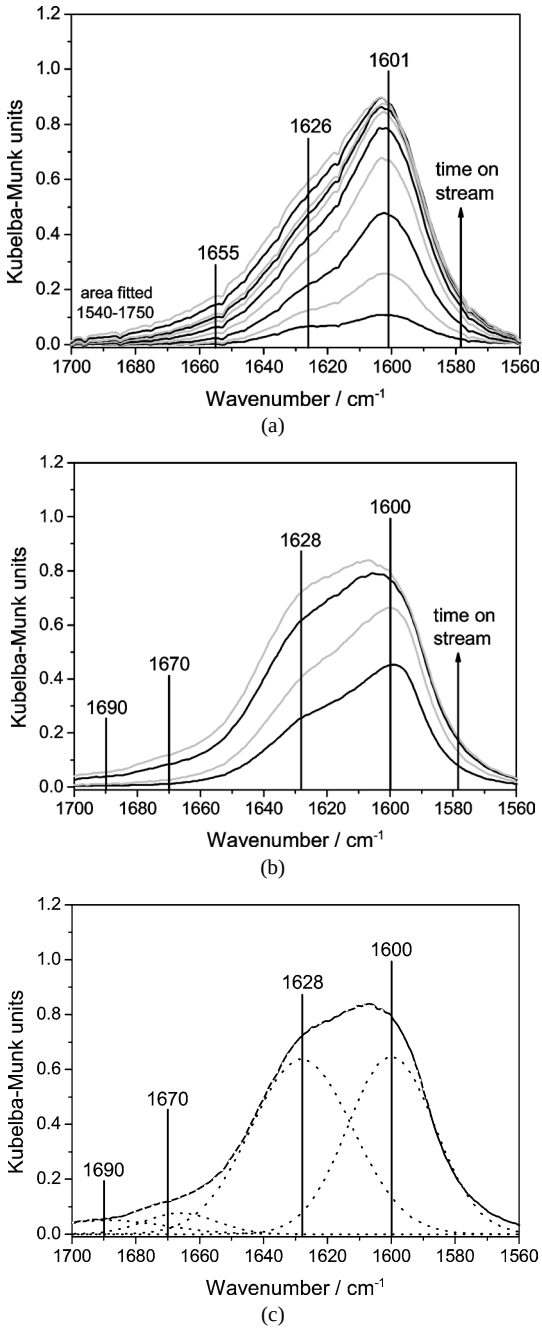

Fig. 7. Kubelka–Munk representation of diffuse reflectance IR spectra after subtraction of linear background (range 1700–1560 cm^{-1}). (a) SZ at 358 K (activated in N_2) and (b) MnSZ at 323 K (activated in O_2) during *n*-butane isomerization; (c) Gauss fit with 4 individual bands of MnSZ spectrum.

and 7b. This species is thus clearly associated with the induction period. It has often been hypothesized that the induction period is due to "buildup of olefins on the catalyst surface" [25]. Although the time-on-stream evolution of our species suggests it could be such a postulated intermediate, there is no indication yet that it is not water and thus is a side product of an initiation reaction. The frequency is very close to that of gaseous water, which is consistent with isolated water molecules (see also the above interpretation from DFT calculations); with increasing time on stream and surface coverage these water molecules will associate with other water or hydrocarbon molecules and the frequency will change, meaning the band at 1600 cm^{-1} may stop growing or even shrink.

Assuming that each molecule of water or of any other species is equivalent to the formation of one surface intermediate from *n*-butane, the band areas can be taken as a measure of the number (concentration) of these active surface species. If the formed surface species act as active sites for many reaction cycles in a catalytic manner, the rate of isomerization will be proportional to the concentration, that is proportional to the total band area increase relative to the starting value. It has also been proposed that during the initial phase of high activity of promoted catalysts, processes are stoichiometric rather than catalytic [32]. If each intermediate reacts just once, the rate of isomerization would be proportional to the differential increase in surface species, that is, to the incremental band area.

We attempted to correlate the rate of isobutane formation (during the period of increasing activity) with the area of individual bands or the sum of areas of several bands. There was definitely no correlation between rate and incremental area increase for any of the bands. As all bands increase with time on stream and the rate increases during the induction period, correlations with linear segments were almost always obtained, and the linear correlation extended through most of the data points from the induction period for the two large bands. The band(s) at high frequency were very small, and the areas extracted from the fits were not considered reliable. It was not possible to determine which individual bands were connected to the rate and which were not. If the bands arose from differently associated water species, all of them would indicate formation of an active surface species, and the sum would reflect the total number. The best correlation with the rate was obtained when all bands in the range of 1760–1540 cm^{-1} were considered. Because the baseline is not straight over this range (see Fig. 3b), the minima (in Kubelka–Munk representation) on either side of the group of bands were used as integration limits. The area prior to reaction was subtracted; that is, the isomerization rate was plotted versus the area increase. Such correlations are shown in Fig. 8 for SZ and MnSZ. For SZ (358 K and 1 kPa *n*-butane) the conversion was low and the rate data, which scattered somewhat, were smoothed for this analysis. A linear correlation results in the case of SZ, which is consistent with observations by Li et al. [80]. At 378 K and

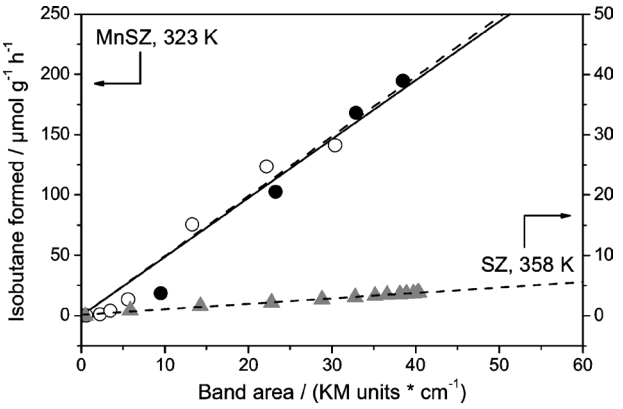

Fig. 8. Rate of isomerization vs area increase of bands in the range 1760–1540 cm^{-1} for SZ and two different MnSZ catalysts. Reaction conditions: 1 kPa *n*-butane.

5 kPa *n*-butane, a steeper slope resulted (roughly 10 times as steep; not shown). For MnSZ, the rate of isomerization also increased with the area of the feature in the IR spectra, but the data show deviations from linearity, and linear regressions do not necessarily pass through the origin. Possible reasons for this might be the following. Seemingly small initial rates may be caused by hindered product desorption at a low reaction temperature or a delay of the gas-phase analysis relative to the events in the DRIFTS cell, which becomes evident only when the performance changes rapidly. Toward the end of the induction period, the rate may already be reduced by deactivation, because in contrast to SZ, MnSZ deactivates. All of these arguments are also valid in case of FeSZ, which changes performance even faster than MnSZ. Indeed, rate and IR data seemed uncorrelated in the case of FeSZ.

A linear correlation of the isomerization rate with the amount of water is consistent with the hypothesis of an ODH initiation reaction. However, water is only one out of three products of ODH. There is so far no proof of an adsorbed butene or a species formed from it, unless one or more of the bands arise from C=C vibrations. Reduction of a catalyst component is also not evident, whereby only reduction of sulfate and not of zirconium or a promoter may be detectable by IR spectroscopy. Furthermore, it cannot be determined whether water is formed by ODH or in a secondary reaction after protonation of the alkane, that is, through oxidation of the hydrogen in statu nascendi from the decay of an alkanium ion.

There is a considerable difference between SZ and MnSZ in the slopes (Fig. 8). Assuming equal extinction coefficients of the same bands for the two catalysts, a faster turnover per active surface species is observed for the promoted catalyst. The reaction temperature is lower for the promoted catalyst, but this should cause a flatter slope. The isomerization rate should be lower at lower temperature, and more of the formed water should accumulate on the surface (and not desorb) than at higher temperature. Hence, the difference between the two catalysts may in reality be even larger.

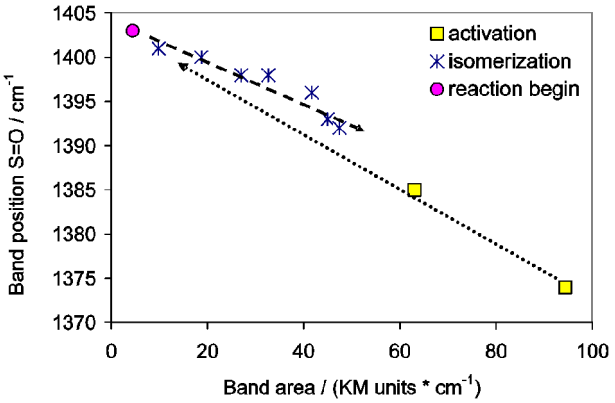

Fig. 9. Correlation of position of S=O double bond stretching vibration around 1400 cm^{-1} with area of bands in the range 1760–1540 cm^{-1}. Arrows indicate course of time: band area decreases during activation with concomitant shift of S=O band to higher wavenumbers, reverse behavior during reaction.

The result demonstrates that independently of the initiation reaction, promoted catalysts exhibit a faster intrinsic isomerization rate. The total amounts of water formed on either of the catalysts in the two experiments shown in Fig. 8 are comparable, indicating no significant difference in the number of sites capable of initiation. Considering also our observations of the Mn valence, which does not change in any particular way during the induction period [19], the role of the promoters seems to be acceleration of the isomerization cycle.

The position of one of the S=O vibrations changed during the course of the reaction, indicating modifications to structure or environment of the sulfate. This band, according to the literature located at 1400–1370 cm^{-1} depending on sample and pretreatment, is known to shift upon adsorption of polar molecules; for example, pyridine or CO cause shifts of up to −81 [81] or −31 cm^{-1} [82], respectively. In our experiments, this band had shifted upward during pretreatment (i.e., dehydration of the catalyst) and shifted downward during reaction. In Fig. 9 the shift of the S=O double bond stretching vibration is plotted against the area of the bands in the range of 1760–1540 cm^{-1} for the SZ catalyst. There seems to be a linear correlation, although the change in the S=O band position for SZ is small and the slopes are shallow. One interpretation of the almost identical slope for the activation and for the reaction branch is that the shift during reaction is only caused by water and not by any other surface species, such as a hydrocarbon deposit. However, the effect of the very polar water molecule may overpower the effect of a second species. For promoted SZ, the shift of the S=O band is about 1.5 times larger than for SZ at equal total area of the water bands (not shown). Reasons for this difference between SZ and promoted SZ could be variations in the extinction coefficient for the adsorbed water species, a more easily polarizable sulfate species on the surface of the promoted catalysts, or both.

4.5. Regeneration

Several authors have reported that the activity of SZ [47,51,58] and of promoted SZ [3] catalysts can be fully regenerated by heating in air to 723 K or in O_2 to 753 K. Regeneration in O_2 at 723 K "essentially reproduces" the DRIFT spectrum of freshly activated SZ [49]; furthermore, the Raman spectrum is identical to that of a fresh catalyst after reactivation at 753 K in O_2 [51]. Irreversible changes to the SZ were reported after reaction of longer hydrocarbons such as hexane at a relatively high reaction temperature of 473 K [54]. Formation of H_2S during reaction of *n*-butane at 523 K was reported by Ng and Horvát [83]. Furthermore, Risch and Wolf [40] claimed that to recover the original activity of SZ, treatment in oxygen must be followed by rehydration. Also for promoted SZ, regeneration may fail; for example, Coelho et al. [26] could not recover the high initial activity. Morterra et al. [3] reported that an initial activation of Fe- and Mn-promoted SZ in He produces a material as active as unpromoted SZ, and even subsequent oxidizing treatments cannot generate a highly active catalyst. We could completely reestablish the IR spectrum and the catalytic activity of MnSZ through treatment at 773 K in O_2. Even when the catalyst was first activated in N_2 and then regenerated in O_2, we reached, as indicated by spectra and performance, the same state as after activation or repeated regeneration in O_2. Obviously, neither the treatments at 773 K nor the isomerization reaction at 323 K cause irreversible changes to the material. One potential explanation for the discrepancy to Morterra's results is the difference in composition; his catalyst also contained Fe.

The spectrum of the deactivated MnSZ is dominated by bands of adsorbed water. On this broad background, very weak bands of hydrocarbon species are visible in the CH stretching vibration region. After a regeneration attempt in N_2, pronounced bands of hydrocarbon deposits are detected. Two bands at 1533 and 1465 cm^{-1} indicate conjugated C=C stretching and CH bending (position not specific for unsaturated or saturated species) vibrations. Therefore, small amounts of hydrocarbons must have remained on the surface after reaction, although the system was purged for 1 h in N_2 before heating for regeneration, and these species undergo dehydrogenation to unsaturated compounds. According to the literature, removal of coke through heating in inert gas [34] is possible, but according to Li and Gonzalez it is accompanied by SO_2 evolution [49]. The reflectance in the region of the fundamental sulfur–oxygen vibrations is so low that changes in sulfate content may not lead to a measurable change in intensity. But the sulfur–oxygen overtones and combination modes are almost congruent in the spectra of the activated and the "regenerated" MnSZ (Fig. 6a). Hence, we have no evidence for significant sulfur loss during the treatment in N_2. This result seemingly contrasts the observation by Li and Gonzalez [49] of SO_2 evolution upon heating of the deactivated catalysts in N_2, but they had conducted the isomerization at 473 K with 10 kPa *n*-butane, and presum-

ably more and different coke species formed than under our mild reaction conditions. In light of our observations and the literature data, it appears that SZ catalysts are irreversibly damaged when exposed to trace amounts of hydrocarbons—even contaminations in a feed delivery system—at too high a temperature.

The fact that MnSZ "regenerated" in N_2 is completely inactive, although the sulfate pattern in the IR is equal to that of activated MnSZ merits some consideration. Because sulfate is a prerequisite for isomerization activity, it is assumed that it is part of the active site. It has been proposed that only 20% of the sulfate is involved in adsorption of the reactant, and only 2% act as reaction sites [44]. A change of a small fraction (2%) of sulfate species would be difficult to discern because slight changes in the DRIFT spectra can arise from small variations in treatment (compare Figs. 4a and 4b). In other words, the poisoning by the deposits is not reflected in the spectral signature of the sulfate either because the number of sites blocked is too small, or these sites are not directly connected to the sulfate.

5. Conclusions

All bands in the IR spectra obtained in situ after activation of sulfated zirconia and Fe- or Mn-promoted sulfated zirconia have been assigned with the help of DFT results from the literature. The predominant species in this state on all catalysts is an $S_2O_7^{2-}$ configuration. The surface is still partially hydrated, with an estimated water content of 60–125 µmol g^{-1}. Strong Lewis acid sites capable of adsorbing N_2 at temperatures up to 358 K are present.

Experiments with activation in N_2 or O_2 demonstrate that the state of the surface functional groups (hydroxyl and sulfate) of manganese-promoted sulfated zirconia is independent of the atmosphere, whereas the reaction profile is not. Complete regeneration of the catalytic and spectroscopic properties can be achieved in O_2. In N_2, the spectral signature of the hydroxyl and sulfate groups is recovered, but the material is rendered inactive. Both of these observations indicate that it is impossible to predict catalytic activity solely from the state of the functional groups.

Spectroscopic evidence is presented for the accumulation of certain species on the surface during the phase of rising conversion (induction period) in *n*-butane isomerization. Several bands are observed between 1760 and 1540 cm^{-1} and at 5200 cm^{-1}, indicating adsorbed water, potentially a product of oxidative dehydrogenation, but maybe also other species. At early times on stream, before maximum conversion is reached, the rate of isomerization is proportional to the area of the bands in the region of 1760–1540 cm^{-1}. Hence, the absorbing species must be active intermediates or side products of the reaction producing the intermediates. It follows that the rate during the induction period depends on two factors: the number of active surface species formed and the intrinsic turnover per such species. The presence of manganese enhances this intrinsic turnover frequency. So far it has been believed that promoters such as iron or manganese facilitate the reaction initiation; here, for the first time, an effect of a promoter on the isomerization itself is proven.

Acknowledgments

The authors thank Gisela Lorenz for help with the preparation of the catalysts, Edith Kitzelmann for recording the diffractograms, Rolf E. Jentoft for acquiring the thermogravimetric data, and Nadja Maksimova for measuring the nitrogen adsorption. Intense discussion with Alexander Hofmann and Joachim Sauer is gratefully acknowledged. Financial support through DFG priority program 1091, "Bridging the gap between real and ideal systems in heterogeneous catalysis" (JE 267/1), is highly appreciated.

References

[1] M. Hino, K. Arata, J. Chem. Soc., Chem. Commun. (1980) 851–852.
[2] C.-Y. Hsu, C.R. Heimbuch, C.T. Armes, B.C. Gates, J. Chem. Soc., Chem. Commun. (1992) 1645–1646.
[3] C. Morterra, G. Cerrato, S. Di Ciero, M. Signoretto, A. Minesso, F. Pinna, G. Strukul, Catal. Lett. 49 (1997) 25–34.
[4] J.E. Tábora, R.J. Davis, J. Chem. Soc., Faraday Trans. 91 (12) (1995) 1825–1833.
[5] T. Tanaka, T. Yamamoto, Y. Kohno, T. Yoshida, S. Yoshida, Jpn. J. Appl. Phys. 38 (1999) 30–35.
[6] T. Yamamoto, T. Tanaka, S. Takenaka, S. Yoshida, T. Onari, Y. Takahashi, T. Kosaka, S. Hasegawa, M. Kudo, J. Phys. Chem. B 103 (1999) 2385–2393.
[7] W.E. Alvarez, H. Liu, D.E. Resasco, Appl. Catal. A: Gen. 162 (1997) 103–119.
[8] V. Adeeva, J.W. de Haan, J. Jänchen, G.D. Lei, V. Schünemann, L.J.M. van de Ven, W.M.H. Sachtler, R.A. van Santen, J. Catal. 151 (1995) 364–372.
[9] V. Adeeva, G.D. Lei, W.M.H. Sachtler, Appl. Catal. A: Gen. 118 (1994) L11–L15.
[10] V. Adeeva, H.-Y. Liu, B.-Q. Xu, W.M.H. Sachtler, Top. Catal. 6 (1998) 61–76.
[11] T.-K. Cheung, J.L. d'Itri, B.C. Gates, J. Catal. 151 (1995) 464–466.
[12] A. Jatia, C. Chang, J.D. MacLeod, T. Okubo, M.E. Davis, Catal. Lett. 25 (1994) 21–28.
[13] X. Song, K.R. Reddy, A. Sayari, J. Catal. 161 (1996) 206–210.
[14] A. Sayari, Y. Yang, X. Song, J. Catal. 167 (1997) 346–353.
[15] A. Sayari, Y. Yang, J. Catal. 187 (1999) 186–190.
[16] R. Srinivasan, R.A. Keogh, A. Ghenciu, D. Fărcaşiu, B.H. Davis, J. Catal. 158 (1996) 502–510.
[17] E.C. Sikabwe, M.A. Coelho, D.E. Resasco, R.L. White, Catal. Lett. 34 (1995) 23–30.
[18] R. Srinivasan, R.A. Keogh, B.H. Davis, Appl. Catal. A: Gen. 130 (1995) 135–155.
[19] R.E. Jentoft, A. Hahn, F.C. Jentoft, T. Ressler, J. Synchrotron Rad. 8 (2001) 563–565.
[20] C. Miao, W. Hua, J. Chen, Z. Gao, Catal. Lett. 37 (1996) 187–191.
[21] C.-H. Lin, C.-Y. Hsu, J. Chem. Soc., Chem. Commun. (1992) 1479–1480.
[22] D.R. Milburn, R.A. Keogh, D.E. Sparks, B.H. Davis, Appl. Surf. Sci. 126 (1998) 11–15.
[23] S.X. Song, R.A. Kydd, Catal. Lett. 51 (1998) 95–100.

[24] M. Scheithauer, E. Bosch, U.A. Schubert, H. Knözinger, F.C. Jentoft, B.C. Gates, B. Tesche, J. Catal. 177 (1998) 137–146.
[25] M.A. Coelho, D.E. Resasco, E.C. Sikabwe, R.L. White, Catal. Lett. 32 (1995) 253–262.
[26] M.A. Coelho, W.E. Alvarez, E.C. Sikabwe, R.L. White, D.E. Resasco, Catal. Today 28 (1996) 415–429.
[27] K.T. Wan, C.B. Khouw, M.E. Davis, J. Catal. 158 (1996) 311–326.
[28] M. Benaissa, J.G. Santiesteban, G. Diaz, M. Jose-Yacaman, Surf. Sci. 364 (1996) L591–L594.
[29] E.A. García, E.H. Rueda, A.J. Rouco, Appl. Catal. A: Gen. 210 (2001) 363–370.
[30] K. Arata, Appl. Catal. A: Gen. 146 (1996) 3–32.
[31] J.C. Yori, J.M. Parera, Appl. Catal. A: Gen. 147 (1996) 145–157.
[32] F.C. Lange, T.-K. Cheung, B.C. Gates, Catal. Lett. 41 (1996) 95–99.
[33] F.C. Jentoft, A. Hahn, J. Kröhnert, G. Lorenz, R.E. Jentoft, T. Ressler, U. Wild, R. Schlögl, J. Catal. 224 (2004) 124–137.
[34] C.R. Vera, C.L. Pieck, K. Shimizu, C.A. Querini, J.M. Parera, J. Catal. 187 (1999) 34–49.
[35] S.X. Song, R.A. Kydd, J. Chem. Soc., Faraday Trans. 94 (1998) 1333–1338.
[36] J.M. Millet, M. Signoretto, P. Bonville, Catal. Lett. 64 (2000) 135–140.
[37] R.E. Jentoft, A. Hahn, F.C. Jentoft, T. Ressler, Phys. Scr. T 115 (2005) 794–797.
[38] R.E. Jentoft, A. Hahn, F.C. Jentoft, T. Ressler, submitted for publication.
[39] J.M. Kobe, M.R. González, K.B. Fogash, J.A. Dumesic, J. Catal. 164 (1996) 459–466.
[40] M. Risch, E.E. Wolf, Catal. Today 62 (2000) 255–268.
[41] Z. Hong, K.B. Fogash, J.A. Dumesic, Catal. Today 51 (1999) 269–288.
[42] K.B. Fogash, R.B. Larson, M.R. González, J.M. Kobe, J.A. Dumesic, J. Catal. 163 (1996) 138–147.
[43] R.A. Comelli, C.R. Vera, J.M. Parera, J. Catal. 151 (1995) 96–101.
[44] S.Y. Kim, J.G. Goodwin Jr., D. Galloway, Catal. Today 63 (2000) 21–32.
[45] F.R. Chen, G. Coudurier, J.-F. Joly, J.C. Védrine, J. Catal. 143 (1993) 616–626.
[46] R. Marcus, U. Diebold, R.D. Gonzalez, Catal. Lett. 86 (2003) 151–156.
[47] B. Li, R.D. Gonzalez, Appl. Catal. A: Gen. 174 (1998) 109–119.
[48] B. Li, R.D. Gonzalez, Catal. Today 46 (1998) 55–67.
[49] B. Li, R.D. Gonzalez, Appl. Catal. A: Gen. 165 (1997) 291–300.
[50] F.T.T. Ng, N. Horvát, Appl. Catal. A: Gen. 123 (1995) L197–L203.
[51] D. Spielbauer, G.A.H. Mekhemer, E. Bosch, H. Knözinger, Catal. Lett. 36 (1996) 59–68.
[52] K.B. Fogash, Z. Hong, J.M. Kobe, J.A. Dumesic, Appl. Catal. A: Gen. 172 (1998) 107–116.
[53] H. Knözinger, Top. Catal. 6 (1998) 107–110.
[54] S.R. Vaudagna, R.A. Comelli, N.S. Figoli, Catal. Lett. 47 (1997) 259–264.
[55] G. Resofszki, M. Muhler, S. Sprenger, U. Wild, Z. Paál, Appl. Catal. A: Gen. 240 (2003) 71–81.
[56] S.R. Vaudagna, R.A. Comelli, S.A. Canavese, N.S. Figóli, J. Catal. 169 (1997) 389–392.
[57] C. Li, P.C. Stair, Catal. Lett. 36 (1996) 119–123.
[58] C. Morterra, G. Cerrato, F. Pinna, M. Signoretto, G. Strukul, J. Catal. 149 (1994) 181–188.
[59] L.M. Kustov, V.B. Kazansky, F. Figueras, D. Tichit, J. Catal. 150 (1994) 143–149.
[60] F. Babou, G. Coudurier, J.C. Vedrine, J. Catal. 152 (1995) 341–349.
[61] E.A. Paukshtis, N.S. Kotsarenko, V.P. Shmachkova, Catal. Lett. 69 (2000) 189–193.
[62] I.V. Bobricheva, I.A. Stavitsky, V.K. Yermolaev, N.S. Kotsarenko, V.P. Shmachkova, D.I. Kochubey, Catal. Lett. 56 (1998) 23–27.
[63] M.R. González, K.B. Fogash, J.M. Kobe, J.A. Dumesic, Catal. Today 33 (1997) 303–312.
[64] R. Ahmad, J. Melsheimer, F.C. Jentoft, R. Schlögl, J. Catal. 218 (2003) 365–374.
[65] B.S. Klose, R.E. Jentoft, A. Hahn, T. Ressler, J. Kröhnert, S. Wrabetz, X. Yang, F.C. Jentoft, J. Catal. 217 (2003) 487–490.
[66] A. Hahn, T. Ressler, R.E. Jentoft, F.C. Jentoft, Chem. Commun. (2001) 537–538.
[67] A. Hofmann, J. Sauer, J. Phys. Chem. B 108 (2004) 14652–14662.
[68] A. Hofmann, J. Sauer, personal communication.
[69] M. Benaïssa, J.G. Santiesteban, G. Díaz, C.D. Chang, M. José-Yacamán, J. Catal. 161 (1996) 694–703.
[70] C. Morterra, G. Cerrato, F. Pinna, M. Signoretto, J. Catal. 157 (1995) 109–123.
[71] M. Bensitel, O. Saur, J.-C. Lavalley, B.A. Morrow, Mater. Chem. Phys. 19 (1988) 147–156.
[72] C. Morterra, G. Cerrato, V. Bolis, Catal. Today 17 (1993) 505–515.
[73] T. Riemer, D. Spielbauer, M. Hunger, G.A.H. Mekhemer, H. Knözinger, J. Chem. Soc., Chem. Commun. (1984) 1181–1182.
[74] C. Morterra, G. Cerrato, F. Pinna, M. Signoretto, J. Phys. Chem. B 98 (1994) 12373–12381.
[75] J. Weidlein, U. Müller, K. Dehnicke, Schwingungsspektroskopie, Thieme, Stuttgart, 1988, p. 27.
[76] A.A. Davydov, Kinet. Catal. 20 (1979) 1245–1250.
[77] R.A. Keogh, R. Srinivasan, B.H. Davis, J. Catal. 151 (1995) 292–299.
[78] M.R. González, J.M. Kobe, K.B. Fogash, J.A. Dumesic, J. Catal. 160 (1996) 290–298.
[79] K.M. Neyman, P. Strodel, S.P. Ruzankin, N. Schlensog, H. Knözinger, N. Rösch, Catal. Lett. 31 (1995) 273–285.
[80] X. Li, K. Nagaoka, L.J. Simon, J.A. Lercher, A. Hofmann, J. Sauer, submitted for publication.
[81] A. Patel, G. Coudurier, N. Essayem, J.C. Védrine, J. Chem. Soc., Faraday Trans. 93 (2) (1997) 347–353.
[82] W. Stichert, F. Schüth, S. Kuba, H. Knözinger, J. Catal. 198 (2001) 277–285.
[83] F.T.T. Ng, N. Horvát, Appl. Catal. A: Gen. 123 (1995) L197–L203.